Backbone-Constrained Peptides: Temperature and Secondary Structure Affect Solid-State Electron Transport

Cunlan Guo,[†,§,*] Jingxian Yu,[‡,*] John R. Horsley,[‡] Mordechai Sheves,[†] David Cahen,[†] and Andrew D. Abell[‡]

[†] Department of Materials and Interfaces, Weizmann Institute of Science, Rehovot, 76100, Israel

[‡] ARC Centre of Excellence for Nanoscale BioPhotonics (CNBP), Institute of Photonics and Advanced Sensing (IPAS), Department of Chemistry, The University of Adelaide, Adelaide, SA 5005, Australia

[§] Present address: College of Chemistry and Molecular Sciences, Wuhan University, No. 299 Bayi Road, Wuhan, Hubei 430072, P.R China

Email: cunlanguo@whu.edu.cn; Jingxian.yu@adelaide.edu.au

Phone: +86-2768754085; +61-8-83136694

Table of Contents:

1. Peptide Synthesis

Scheme S1 Synthesis of alkene sidechain

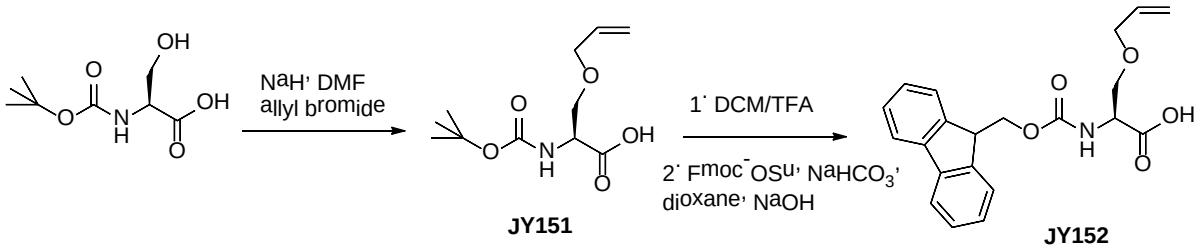

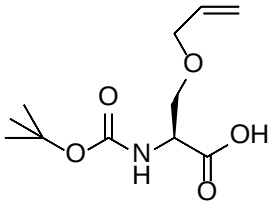

JY151

Boc-Ser-OH (10.48 g, 51.12 mmol) was dissolved in anhydrous DMF (30 mL) and stirred under N_2 at r.t. NaH (60% dispersion in mineral oil (5.08 g)) was suspended in anhydrous DMF (90 mL) and stirred under N_2 over an ice bath (0 ^oC). The Boc-Ser-OH solution was added to the NaH suspension dropwise and the reaction stirred for 30 min. The ice bath was removed and allyl bromide (4 mL) added, and the reaction stirred for a further 3 h. The reaction was then quenched with H_2O (30 mL) and the solvent removed with N_2. The crude residue was dissolved in H_2O (200 mL) and EtOAc (200 mL) and the pH adjusted to pH 2. The organic layer was collected, washed with H_2O and brine, and dried over $MgSO_4$. The solvent was removed *in vacuo* to reveal yellow/brown oil (10.5 g). The crude sample was purified using flash chromatography (eluent EtOAc/petroleum ether: 40% / 60%) to yield pale yellow oil (9.77 g, 78%).

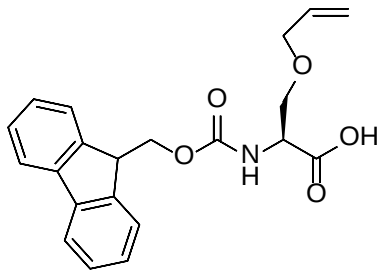

JY152

JY151 (9.77 g, 39.87 mmol) was dissolved in DCM (20 mL) and stirred over an ice bath (0 ^{o}C). TFA (20 mL) was added dropwise and stirred for 30 min. The ice bath was removed and reaction stirred for a further 30 min. The solvent was removed *in vacuo* to reveal a white TFA salt (10.15 g, 39.20 mmol). The Boc-deprotected compound was then dissolved in 1-4 dioxane (55 mL) and one equivalent NaOH (1.56 g, in H_2O (15 mL)) added to neutralize the TFA. $NaHCO_3$ (2 equiv.) and Fmoc-OSu (1 equiv.) were added and the reaction stirred for 12 h. The solvent was removed *in vacuo* and the residue redissolved in $NaHCO_3$ (200 mL, 2.5% w/v), washed with diethyl ether (x3), and acidified to pH2. EtOAc (4 x 200 mL) extractions were performed and the combined organic layers washed with brine and dried over $MgSO_4$. The solvent was removed *in vacuo* to reveal a white solid (12.45 g, 82%). Reverse phase HPLC revealed one peak representative of pure product.

Solid Phase Peptide Synthesis (SPPS)

Peptides **3** and **4** were synthesized using SPPS. Standard Fmoc-based SPPS and commercially available reagents were used for the synthesis of both peptides. 2-Chlorotrityl resin preloaded with Fmoc-Aib-OH (0.80 mmol g^{-1}, 1.0 g, 1 equiv.) was used for both linear peptides. The unreacted active sites on the resin were capped with DCM/MeOH/DIPEA (17:2:1, 2x25 mL) for 30 min and the resin washed with DCM (x3), DMF (x3) and DCM (x3). *N*-Fmoc deprotection was conducted by treating the resin with 25 % piperidine/DMF (25 mL) for 30 min before washing with DCM (x3), DMF (x3) and DCM (x3). Each sequential amino acid was coupled using the following molar ratios of reagents: Fmoc-amino acids were each dissolved in DMF

(20 mL), 1-[bis(dimethylamino)methylene]-1*H*-1,2,3-triazolo[4,5-*b*]pyridinium 3-oxid hexafluorophosphate (HATU)/DMF (0.5 M, 2 equiv.) and DIPEA (4 equiv.). The resin was then washed with DCM (x3) and DMF (x3) followed by DCM (x3), and the coupling procedures repeated. The coupling time was a minimum of 2 h in all cases. Following coupling with the final residue for each linear peptide (3(tritylthio)propionic acid), the resins were washed with DCM (x3), DMF (x3) and DCM (x3) and dried under vacuum. Treatment with 95% TFA/2.5% TIPS/2.5% H_2O (15 mL) for 10 min resulted in cleavage from the resin as well as deprotection of the trityl group from the N-terminal. The filtrate containing each peptide was collected and the TFA removed using N_2. Each peptide was placed under vacuum before being purified using reverse phase HPLC.

Scheme S2 Synthesis of peptide 1

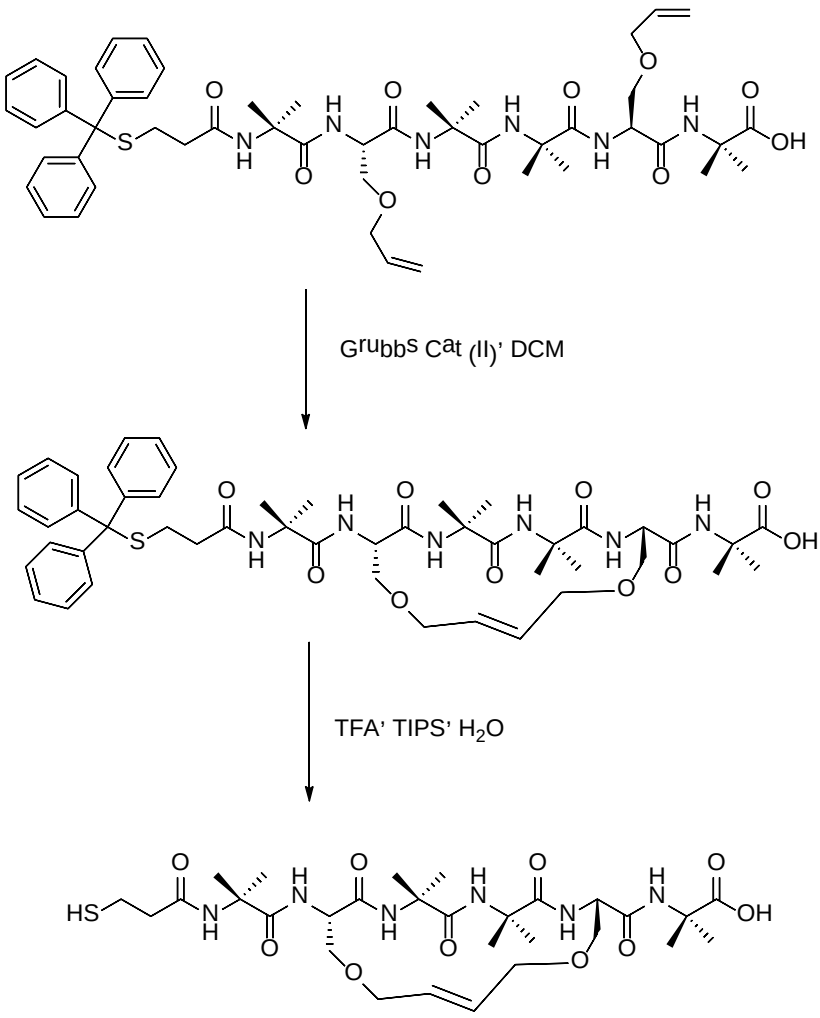

The unsaturated cyclic peptide **1** was prepared from the linear peptide comprising two alkene-containing sidechains described above, using Ring Closing Metathesis (RCM). The linear peptide in this case was cleaved from the resin using 1.5% TFA, so as to retain the trityl protecting group, as shown in Scheme S2 (top). The trityl-protected linear peptide was then purified using column chromatography with EtOAc/petroleum ether (90% / 10%) as the eluent. The purified compound (280 mg, 0.298 mmol) was dissolved in anhydrous DCM (30 mL) and stirred under reflux for a total of 3.5 h at 50 ^{o}C under N_2 atmosphere. A total of 4.5% molar equiv. of Grubbs Cat (II) was used (11 mg, 0.013 mmol), which was divided into three batches of 1.5% molar equiv. (3x 3.7 mg). The first batch was dissolved in anhydrous DCM (500 µL) and added as soon as the peptide solution had reached 50 ^{o}C. After 1 h, the next batch was added,

with the final batch added after 2 h. The reaction solution was stirred under N_2 for a further 1.5 h, and allowed to cool to rt. Activated charcoal (110 mg) was added and the reaction stirred for 72 h. The mixture was then vacuum filtered through celite and the filtrate washed with DCM (x3) and MeOH (x3). The solvent was removed *in vacuo* to reveal crude brown oil (270 mg), which was purified using column chromatography (DCM/MeOH (95% / 5%)). The trityl group was removed using 95% TFA/2.5% TIPS/2.5% H_2O (15 mL) for 1 h. The crude residue was purified using reverse phase HPLC to reveal a white solid, which was used for conductance measurements.

Scheme S3 Synthesis of peptide 2

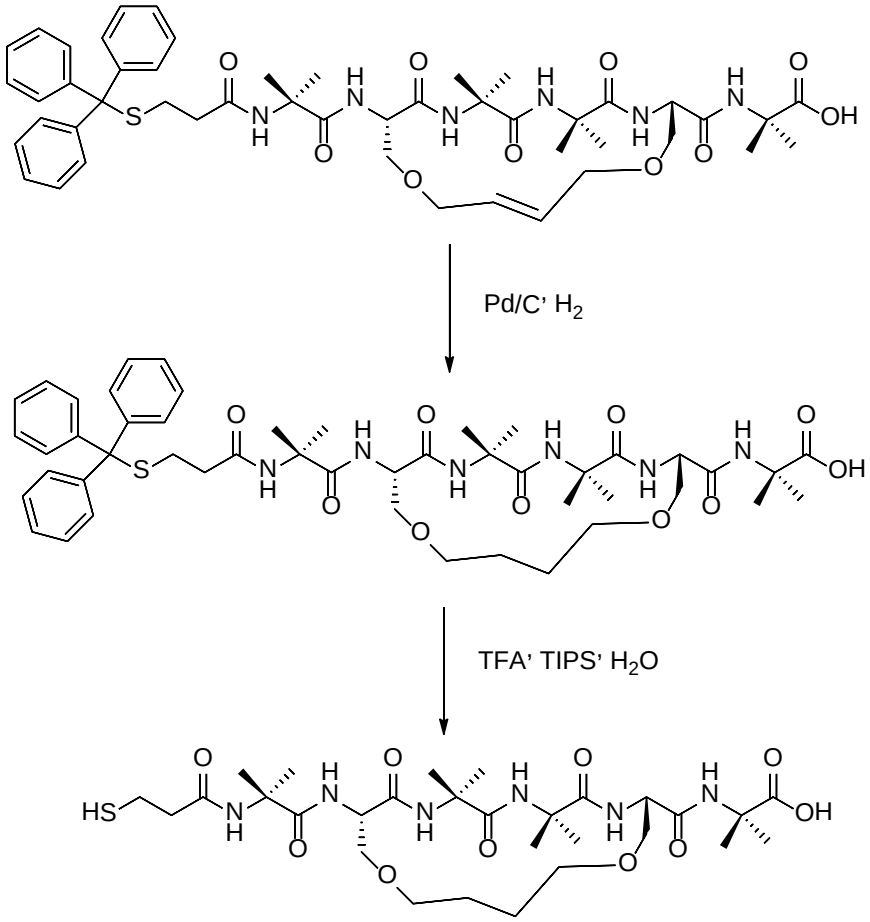

The purified trityl-protected unsaturated peptide (Scheme S3, top) was dissolved in EtOAc and Pd/C (10% w/w) was added. The reaction mixture was stirred and exposed to H_2 gas for 16 h. The solvent was filtered through celite and the filtrate washed with DCM (x3) and MeOH (x3) to reveal crude product, which was treated with 95% TFA/2.5% TIPS/2.5% H_2O (3 mL) for 1 h to remove the trityl group. The TFA was removed by N_2, and the crude product purified using reverse phase HPLC and used for conductance measurements.

2. NMR and MS data for peptides 1-4

Peptide 1 ^{1}H NMR (600 MHz, DMSO-d6) δ 8.30 (s, 1H, NH Aib1), δ 8.10 (s, 1H, NH Aib2), δ 7.94 (m, 1H, NH sidechain1), δ 7.72 (s, 1H, NH Aib3), δ 7.51 (m, 1H, NH sidechain2), δ 7.44 (s, 1H, NH Aib4), δ 5.63– δ 5.61 (m, 2H, OCH_2CHCH), δ 4.50 – δ 4.47 (m, 1H, CαH sidechain1), δ 4.25 – δ 4.22 (m, 1H, CαH sidechain2), δ 4.12 (d, 1H, OC*H*HCH, *J* = 13.3 Hz), δ 4.01 – δ 3.94 (m, 3H, $CαHCH_2O$ sidechain1, $CαHCH_2OCHH$ sidechain2), δ 3.88 – δ 3.85 (m, 1H, $CαHCH_2OCHH$ sidechain2), δ 3.75 – δ 3.72 (m, 1H, OCH*H*CH), δ 3.66 – δ 3.57 (m, 4H, $CαHCH_2O$ sidechain2, CH_2CH_2SH), δ 3.13 – δ 3.09 (m, 2H, CH_2CH_2SH), δ 1.35 – δ 1.29 (m, 24H, 8xCH_3); ^{13}C NMR (600 MHz, DMSO-d6) δ 175.04, 174.72, 174.46. 174.00, 171.13, 168.24, 129.62, 128.40, 56.35, 56.15, 55.82, 54.86, 53.52, 28.81, 28.69, 28.56, 27.30, 26.59, 25.57, 24.91, 24.64, 24.51, 23.30, 22.76, 22.08, 19.73, 18.05, 16.72, 12.44.
HRMS $[M+H]^+$ calc'd = 673.3231, $[M+H]^+$ found = 673.3252.

Peptide 2 ^{1}H NMR (600 MHz, DMSO-d6) δ 8.27 (s, 1H, NH Aib), δ 8.04 (s, 1H, NH Aib), δ 7.92 (d, 1H, NH, *J* = 7.2 Hz), δ 7.55 (s, 1H, NH Aib), δ 7.47 (m, 1H, NH Aib), δ 7.43 (d, 1H, NH, *J* = 6.4 Hz), δ 4.59– δ 4.56 (m, 1H, CαH), δ 4.36 – δ 4.32 (m, 1H, CαH), δ 4.03 – δ 4.00 (m, 1H, CαHC*H*HO), δ 3.89 – δ 3.86 (m, 1H CαHCH*H*O), δ 3.64 – δ 3.55 (m, 4H, $CαHCH_2O$, CH_2CH_2SH), δ 3.15 – δ 3.12 (m, 2H, CH_2CH_2SH), δ 2.19 – δ 2.17 (m, 2H, OCH_2CH_2), δ 2.02 – δ 1.99 (m, 2H, OCH_2CH_2), δ 1.48 – 1.44 (m, 4H, 2xOCH_2CH_2), δ 1.34 – δ 1.27 (m, 24H, 8xCH_3).
HRMS $[M+H]^+$ calc'd = 675.3387, $[M+H]^+$ found = 675.6076.

Peptide 3 ^{1}H NMR (500 MHz, DMSO-d6) δ 8.43 (s, 1H, NH Aib1), δ 8.00 (s, 1H, NH Aib2), δ 7.89 (d, 1H, NH sidechain1, *J* = 5.9 Hz), δ 7.44 (s, 1H, NH Aib4), δ 7.42 (m, 1H, NH Aib3), δ 7.39 (m, 1H, NH alanine), δ 5.88– δ 5.81 (m, 1H, OCH_2CHCH_2), δ 5.23 (d, 1H, OCH_2CHCHH, *J* = 17.3 Hz), δ 5.13 (d, 1H, OCH_2CHCHH, *J* = 10.4 Hz),), δ 4.16 – δ 4.12 (m, 1H, CαH sidechain), δ 4.05 – δ 4.00 (m, 1H, CαH alanine), δ 3.97 – δ 3.92 (m, 2H, OCH_2CHCH_2), δ 3.71 – δ 3.64

(m, 2H, CαHCH_2O), δ 2.75 – δ 2.65 (m, 2H, CH_2CH_2SH), δ 2.49 – δ 2.44 (m, 1H, C*H*HCH_2SH), δ 2.32 – δ 2.29 (m, 1H, CH*H*CH_2SH), δ 1.75 – δ 1.70 (m, 1H, SH), δ 1.37 – δ 1.31 (m, 24H, 8xCH_3), δ 1.25 (m, 3H, CH_3, alanine).

HRMS $[M+H]^+$ calc'd = 645.3282, $[M+H]^+$ found = 645.3222.

Peptide 4 ^{1}H NMR (600 MHz, DMSO-d6) δ 8.47 (s, 1H, NH Aib1), δ 8.04 (s, 1H, NH Aib2), δ 7.93 (d, 1H, NH sidechain1, *J* = 5.6 Hz), δ 7.50 (s, 1H, NH Aib4), δ 7.48 (s, 1H, NH Aib3), δ 7.42 (m, 1H, NH sidechain2), δ 5.86 – δ 5.82 (m, 2H, 2xOCH_2CHCH_2), δ 5.25 – δ 5.09 (m, 4H, 2xOCH_2CHCH_2), δ 4.23 – δ 4.20 (m, 1H, CαH sidechain2), δ 4.13 – δ 4.10 (m, 1H, CαH sidechain1), δ 3.95 – δ 3.93 (m, 4H, 2xOCH_2CHCH_2), δ 3.71 – δ 3.64 (m, 4H, 2x CαHCH_2O), δ 2.69 – δ 2.65 (m, 2H, CH_2CH_2SH), δ 2.51 – δ 2.47 (m, 1H, C*H*HCH_2SH), δ 2.32 – δ 2.29 (m, 1H, CH*H*CH_2SH), δ 1.36 – δ 1.33 (m, 24H, 8xCH_3); ^{13}C NMR (600 MHz, DMSO-d6) δ 175.08, 174.72, 173.92, 171.38, 170.65, 135.13, 134.83, 116.28, 116.10, 70.96, 70.84, 69.19, 68.05, 56.19, 56.04, 55.79, 54.78, 27.68, 26.53, 25.61, 24.74, 24.68, 24.23, 23.85, 23.33, 19.78.

HRMS $[M+H]^+$ calc'd = 701.3544, $[M+H]^+$ found = 701.3513.

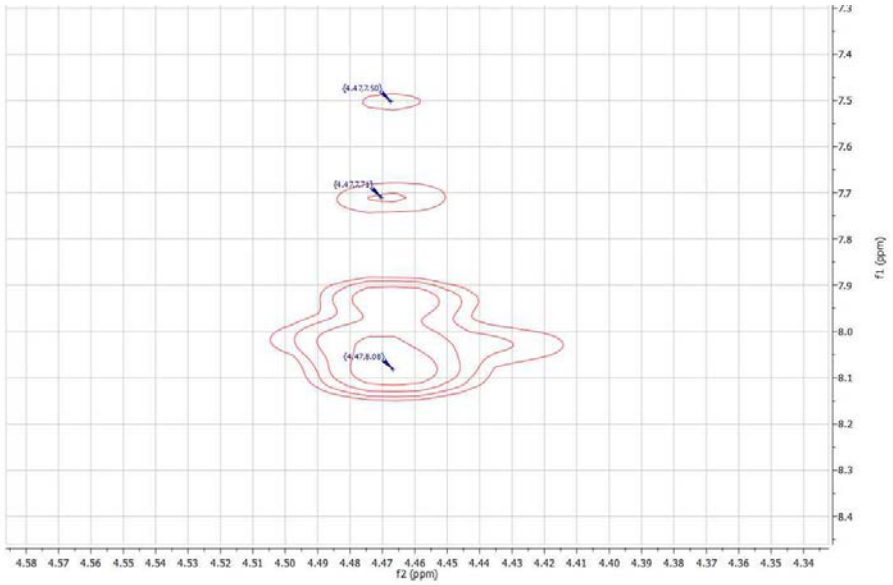

Figure S1. CαH (*i*) to NH (*i*+3) ROESY correlations for peptide **1** indicating the presence of a 3_{10}-helical structure.

3. Computational conformational data for peptides 1-4

Table S1. Dihedral angles for all residues in the lowest energy conformers for peptides **1**-**4**.

	peptide **1**		peptide **2**		peptide **3**		peptide **4**	
	Φ	ψ	Φ	ψ	Φ	ψ	Φ	ψ
Residue 1	-60.336	-30.192	-60.428	-29.753	-59.959	-29.975	-59.892	-30.597
Residue 2	-62.312	-17.854	-62.267	-18.848	-52.231	-32.138	-55.717	-25.606
Residue 3	-51.101	-30.099	-53.249	25.954	-54.688	-29.164	-52.411	-35.026
Residue 4	-53.296	-30.137	-52.338	-29.089	-54.901	26.944	-57.618	-22.224
Residue 5	-69.220	-10.255	-63.394	-17.485	-56.596	-27.593	-60.109	-22.784
Residue 6	-61.497	-25.525	-61.452	-24.811	-61.920	-24.008	-62.109	-24.490

Table S2. Distances critical to the characterization of a 3_{10}-helical peptide.

	Ideal 3_{10}-helical distances (Å)	**peptide 1 (Å)**	**peptide 2 (Å)**	**peptide 3 (Å)**	**peptide 4 (Å)**
CαH (*i*) to NH (*i*+1)	3.4	3.4	3.4	2.9	3.0
$C\beta H_2$ (*i*) to NH (*i*+1)	2.9 – 4.4	3.3 – 4.2	3.2 – 4.1	4.2 – 4.6	4.2 – 4.5

Table S3. Intramolecular hydrogen bond lengths in (Å).

Residue	**peptide 1**	**peptide 2**	**peptide 3**	**peptide 4**
1	2.054	2.073	2.081	2.055
2	2.240	2.223	2.171	2.187
3	2.008	2.059	2.034	1.911
4	2.111	2.084	2.175	2.237
5	2.160	2.108	2.080	2.114
Average	**2.114**	**2.109**	**2.108**	**2.100**

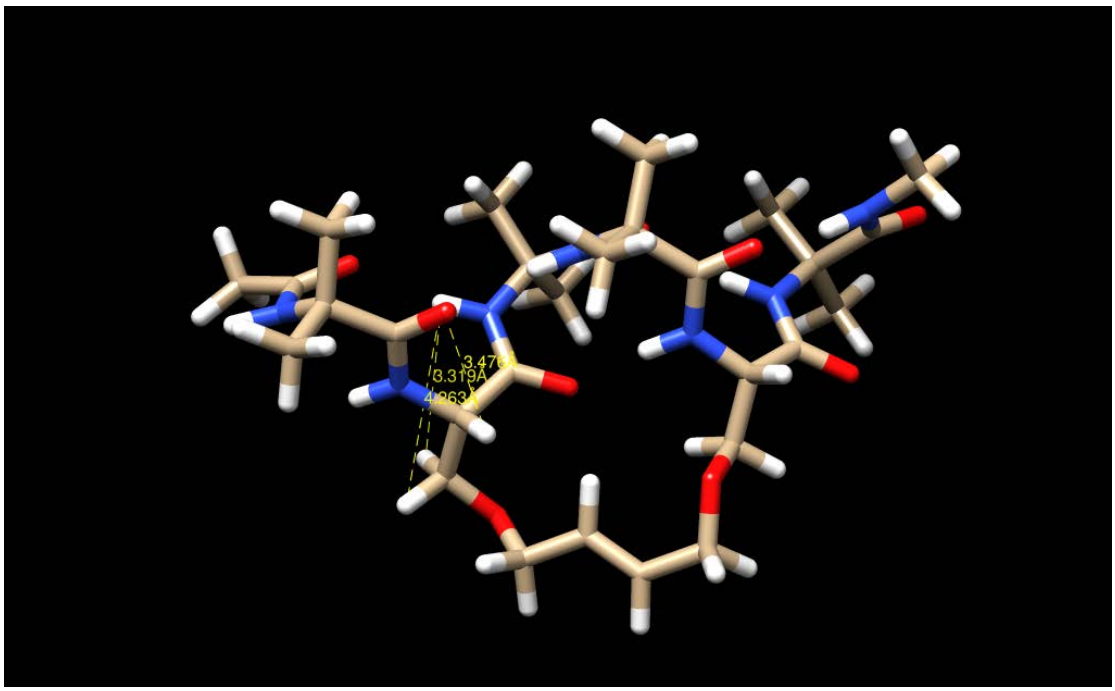

Figure S2. Lowest energy conformer of peptide **1** showing distances for CαH (*i*) to NH (*i*+1) and $C\beta H_2$ (*i*) to NH (*i*+1) interactions.

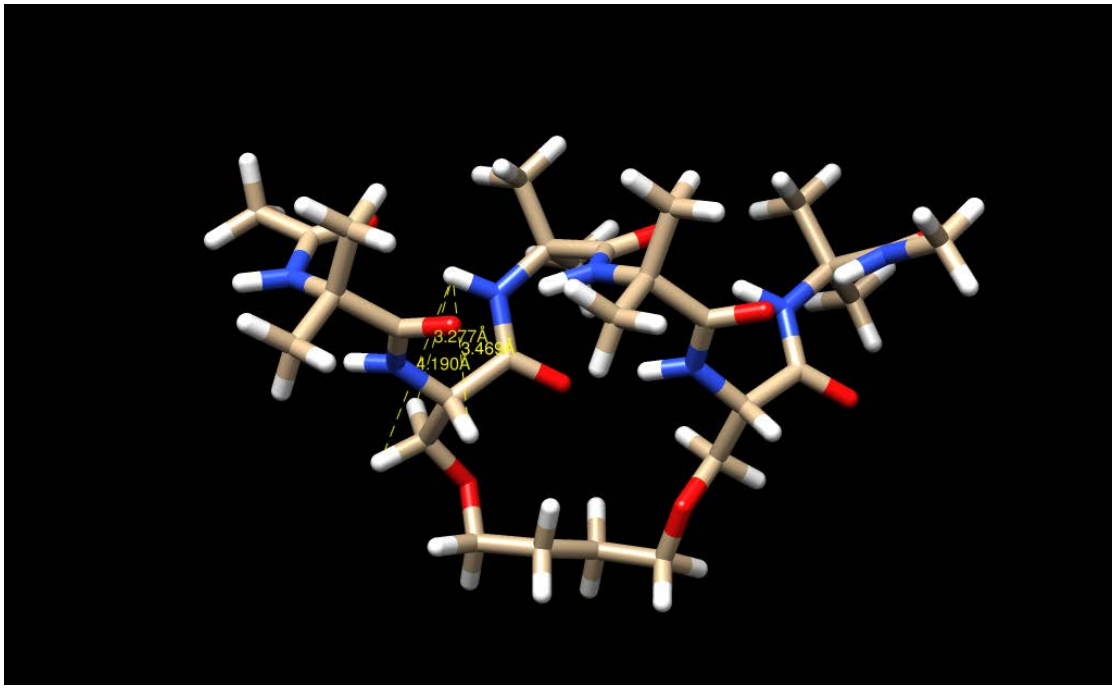

Figure S3. Lowest energy conformer of peptide **2** showing distances for CαH (*i*) to NH (*i*+1) and $C\beta H_2$ (*i*) to NH (*i*+1) interactions.

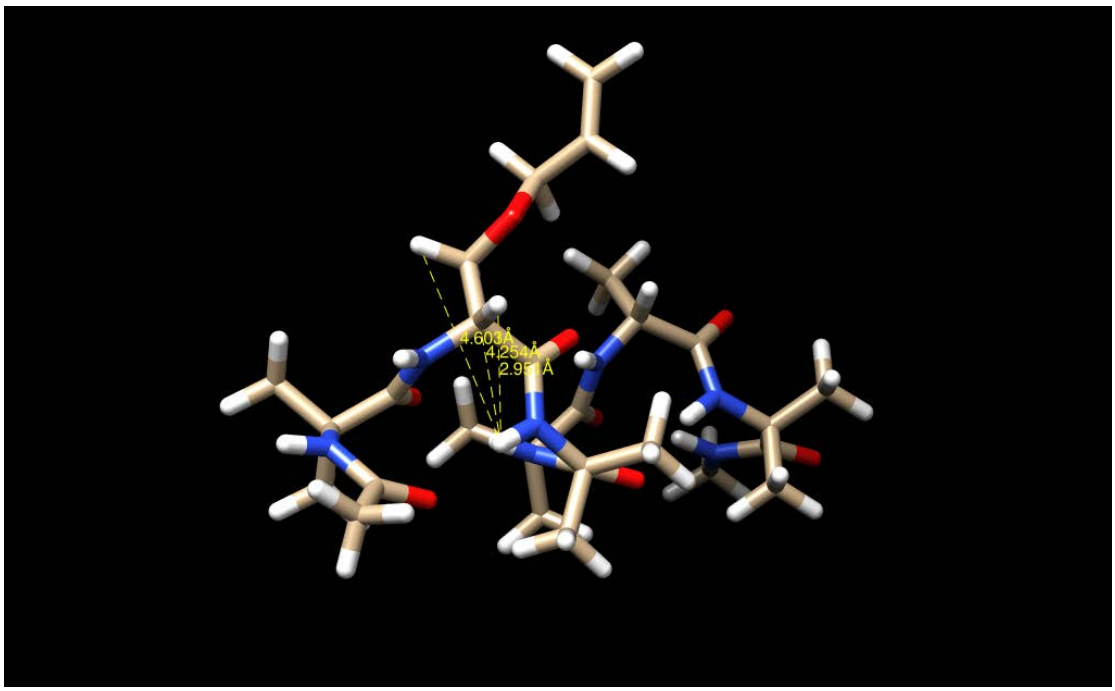

Figure S4. Lowest energy conformer of peptide **3** showing distances for CαH (*i*) to NH (*i*+1) and $C\beta H_2$ (*i*) to NH (*i*+1) interactions.

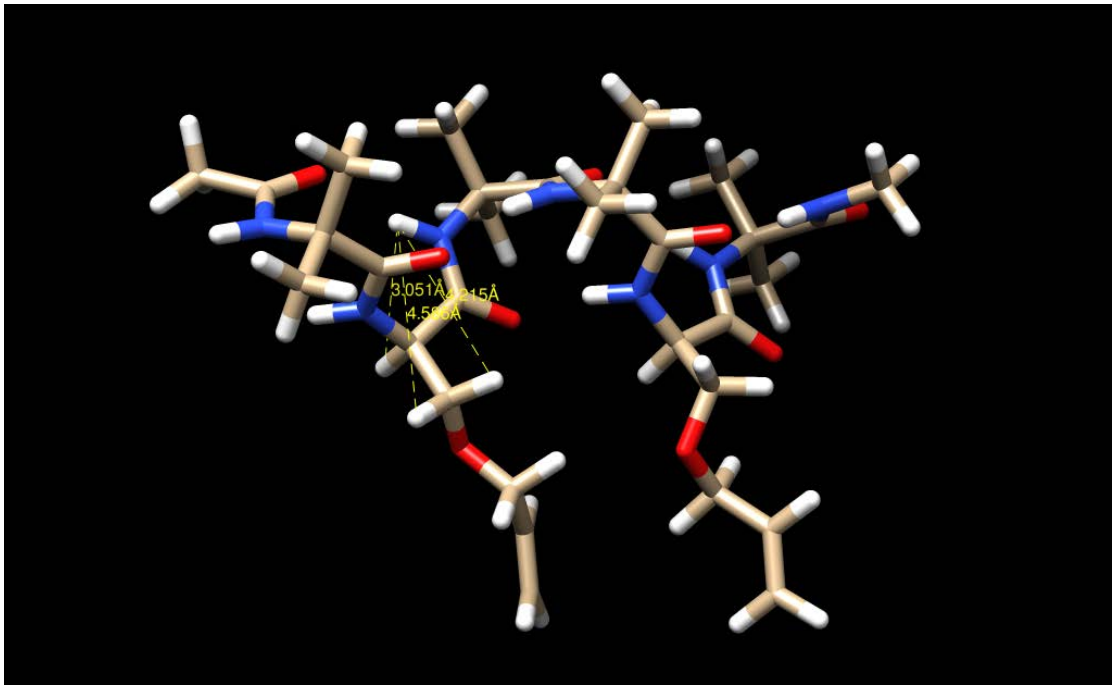

Figure S5. Lowest energy conformer of peptide **4** showing distances for CαH (*i*) to NH (*i*+1) and $C\beta H_2$ (*i*) to NH (*i*+1) interactions.

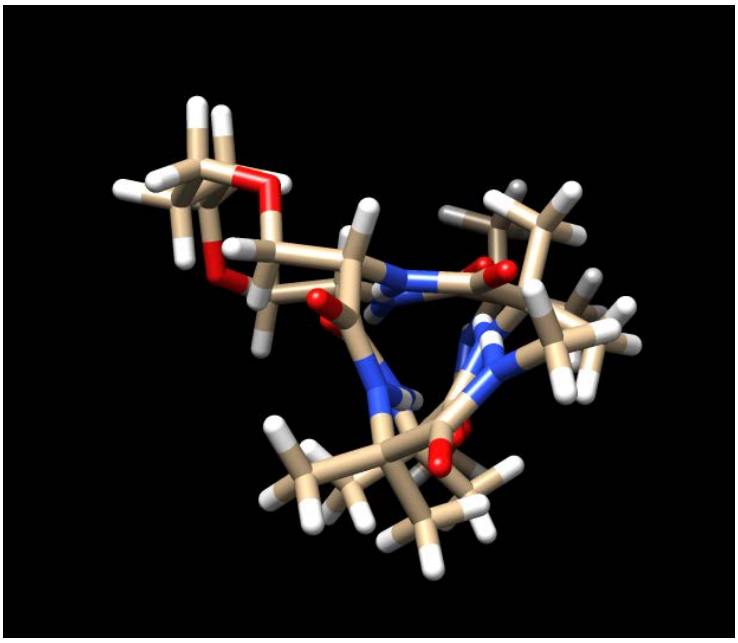

Figure S6. Top view looking down helix showing a triangular-shaped void in the center characteristic of a 3_{10}-helix in peptide **2**.

4. PM-IRRAS, AFM, and ellipsometry data for peptides 1-4

Table S4. Overview of Amide I and Amide II IR absorption peaks for peptide monolayers.

	Amide I (cm^{-1})	Amide II (cm^{-1})	Amide I/II
peptide **1**	1668	1537	3.1
peptide **2**	1669	1538	3.1
peptide **3**	1669	1540	4.08
peptide **4**	1669	1540	3.21

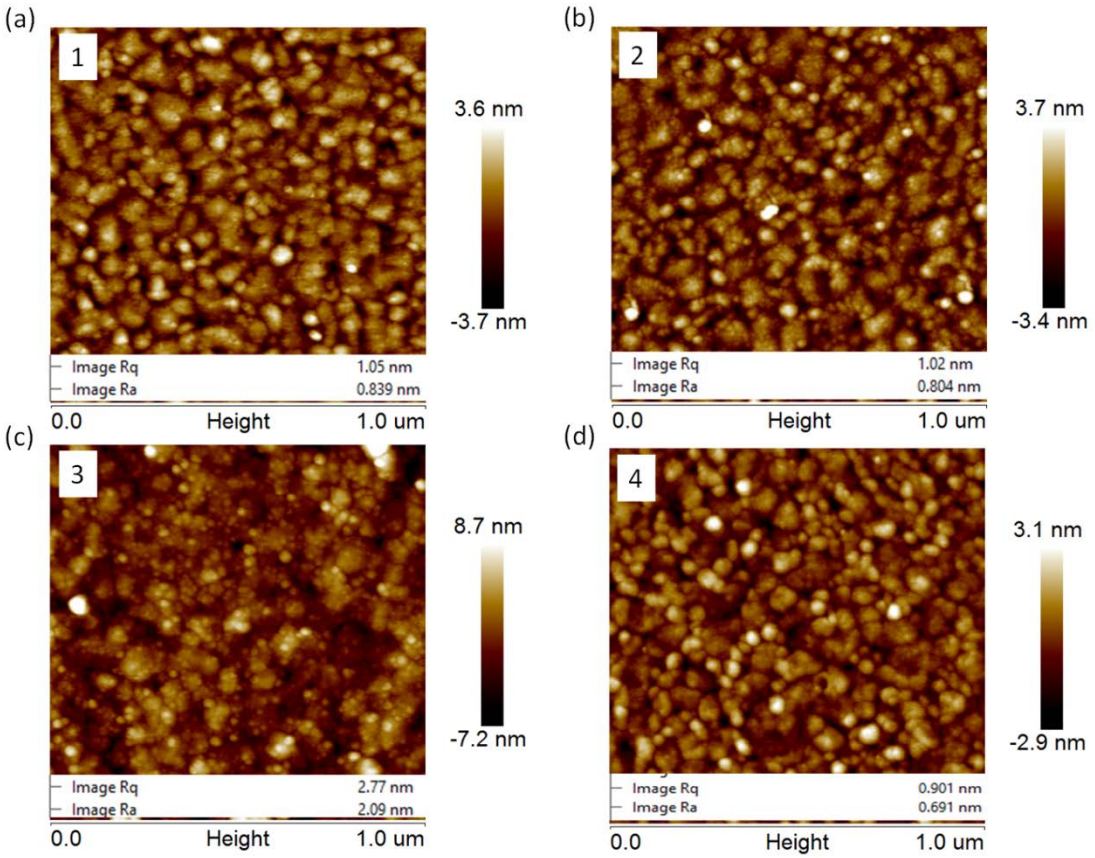

Figure S7. Morphologies of peptide monolayers on Au surface measured by AFM. (a) peptide **1**; (b) peptide **2**; (c) peptide **3**; (d) peptide **4**.

Table S5. Thickness of peptide monolayers measured by ellipsometry.

	peptide **1**	peptide **2**	peptide **3**	peptide **4**
Thickness (Å)	16.8 ± 0.8	17.4 ± 0.79	18.8 ± 0.07	18.0 ± 0.29

5. Temperature-dependent conductance measurements for peptides 1-4

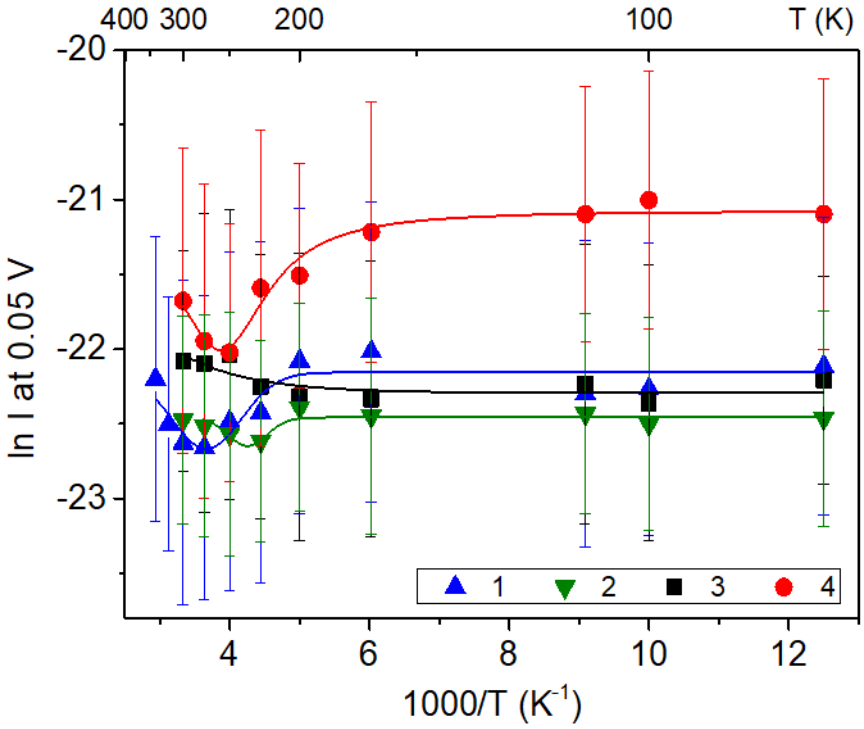

Figure S8. Measured current for peptides **1-4** as a function of temperature ranging between 80 K and 340 K. Error bars indicate the deviations of measured current over 20 junction devices.

6. Temperature-dependent α-helical content of self-assembled peptides 1-4

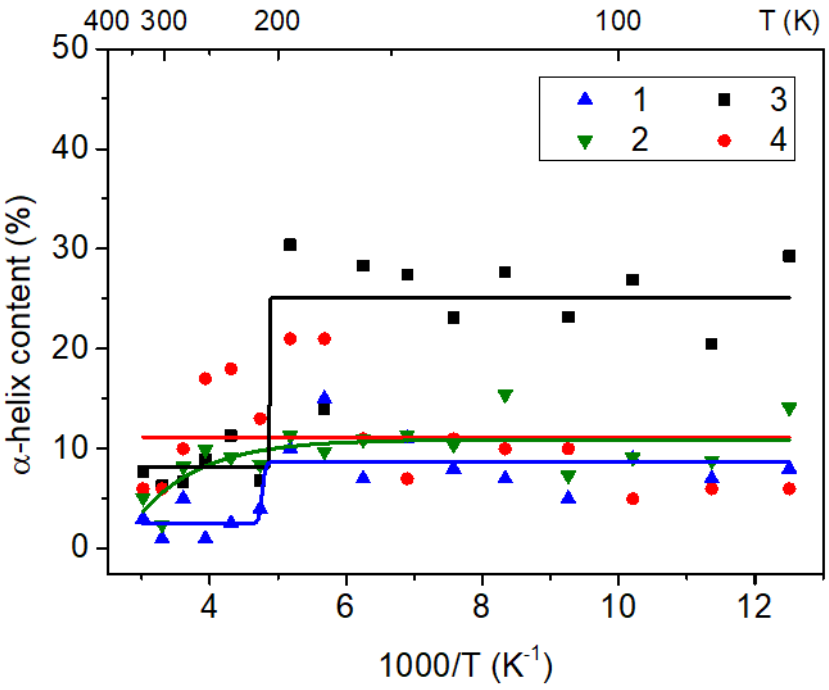

Figure S9. Temperature-dependent α-helical content of self-assembled peptides **1-4**.

7. Analysis of MD data for mobility (RMSF) per residue

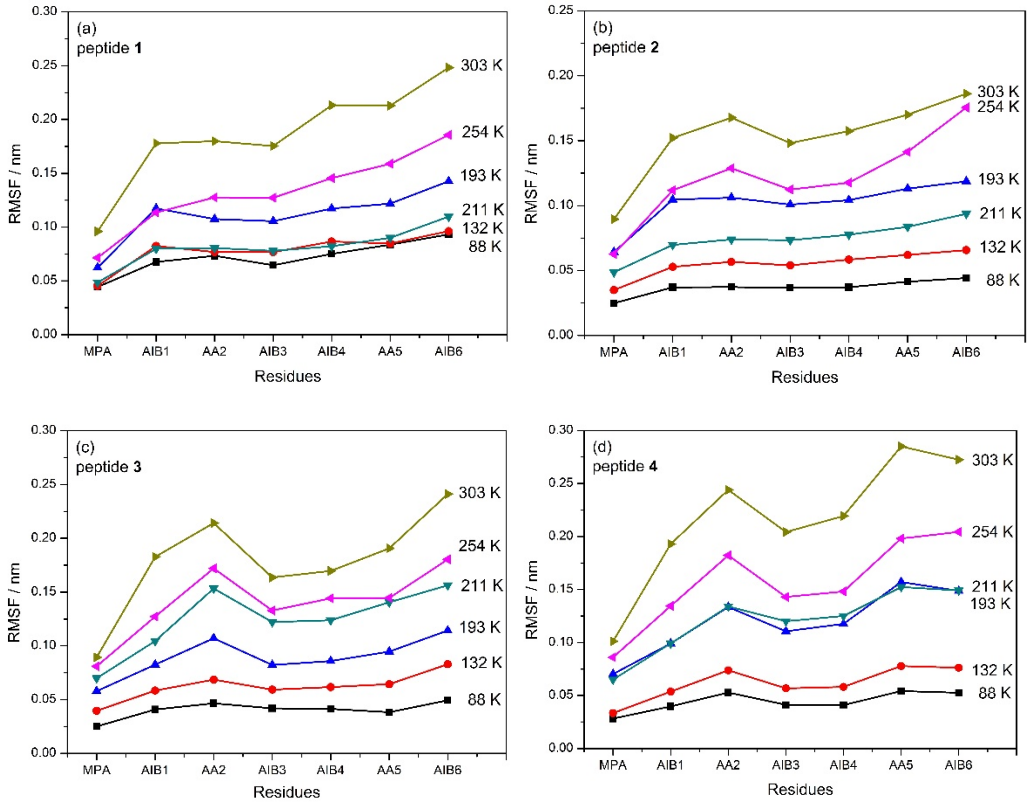

Figure S10. The mobility (RMSF, root mean square fluctuations) per residue around the average position in monolayers containing each of the four peptides at different temperatures.

Figure S10 depicts the mobility of each residue in the peptides around their average positions in the monolayers at different temperatures. At a given temperature, the MPA linker has the lowest RMSF value as it binds to the surface via an Au-S bond, while the residues nearest to the distant C-terminal generally have higher RMSF values. For peptides **1** and **2** which are constrained into a macrocycle by a side bridge, the RMSF value per residue gradually increases with elevating temperature from 88 K to 193 K. However, after increasing to 211 K, a sudden drop in the RMSF values is observed for the two peptides. With the temperature further increasing from 211 K to 303 K, the RMSF values per residue rise again. It is worth noting that the four residues within the macrocycle loop of peptides **1** and **2**, namely the two tethered AA2, AA5, and AIB3, AIB4, each have relatively similar RSMF values for any given temperature, compared to linear peptides **3** and **4**. The collective motions of the

macrocycle induce an accumulated potential energy (dihedral / angle strain) in the loop. This energy build-up is released at approximately 211 K, with the result being a lower 3_{10}-helical content in the peptides. For the linear peptide **3** with an alanine at AA5, the RMSF value per residue rises with increasing temperature, from 211 K to 303 K, with no sudden drop of RMSF values. Peptide **4** with its modified alkene at AA5, has a higher RMSF value per residue than that of **3** throughout the entire sequence, with the modified alkene always having the highest RMSF value in the sequence at any given temperature. This is because the alkene-containing side chain is much longer and more flexible than the alanine one in **3**, and is positioned much further from the surface. This helps explain why the 3_{10}-helical content within peptide **4** is gradually reduced as temperatures increase.